

FATIGUE OF CAST STEELS
PART I-A STUDY OF THE NOTCH EFFECT AND OF THE
SPECIMEN DESIGN AND LOADING ON THE FATIGUE
PROPERTIES OF CAST STEEL

PART II-FRACTOGRAPHIC STUDIES OF
FATIGUE IN CAST STEEL

RESEARCH PROJECTS AT CASE INSTITUTE
OF TECHNOLOGY

Sponsored by

Steel Foundry Research Foundation

CHARLES W. BRIGGS

Director of Research

© by Steel Foundry Research Foundation

Rocky River, Ohio

April, 1967

Published and Distributed by Steel Founders' Society of America
Westview Towers, 21010 Center Ridge Road Rocky River, Ohio 44 116

TABLE OF CONTENTS

	Page
Scope of the Research Report	3
Summary of the Research Report Conclusions	3
Preface	4
Part I - A Study of the Notch Effect and of the Specimen Design and Loading on the Fatigue Properties of Cast Steel	
Section 1 . The Notch Effect on Fatigue of Cast Steel	6
Procedure	6
Effect of Notches in Fatigue	8
Section 2 . The Effect of Specimen Design and Type of Loading on the Fatigue of Cast Steel	10
Plate Bending Fatigue Tests	11
Torsion Fatigue Tests	11
Comparison of Torsion and Bending Fatigue Results	11
Conclusions to Part I of the Research Report	13
Part II- Fractographic Studies of Fatigue in Cast Steel	15
Procedure and Materials	16
Crack Initiation	17
Surface Morphology vs . Microstructure	18
Rate of Crack Propagation and Sensitivity to Crack Initiation	21
Effect of Inclusions	24
Conclusions to Part II of the Research Report	25
Appendix I-Preparation of Replicas	25

STEEL FOUNDRY RESEARCH FOUNDATION FATIGUE OF CAST STEELS

SCOPE OF THE RESEARCH REPORT

The purpose of the research included in this report is to extend the knowledge on the fatigue properties of cast steel by presenting a study of the effect of notches on fatigue properties and the effect of specimen design and the method of loading on the fatigue properties of cast steel.

A further purpose was to examine the fatigue fracture surfaces of cast steel and to study the characteristics of fatigue failure in origin, direction and rate by microscopic analysis through fractography techniques.

SUMMARY OF THE RESEARCH REPORT CONCLUSIONS

Notch Effect-A severe notch (0.015 inch radius) in fatigue testing of cast steel results in a 36 percent reduction in endurance limit based on unnotched specimens. An extremely severe notch (0.001 inch radius) results in a 42 to 53 percent reduction in the endurance limit. The fatigue strength reduction factor K_f for extreme notched specimens is appreciably higher for cast steel in the quenched and tempered condition.

Specimen Design and Loading-Cast steel exhibits better endurance properties in reversed torsion than reversed bending. Bending fatigue tests of cast steel tested at 1800 rpm result in lower endurance properties than rotating beam tests at 10,000 rpm. The difference is greater at the higher tensile strength level.

Fractographic Studies-The rate of fatigue crack propagation in a normalized cast steel is greater than in quenched and tempered cast steel of equal strength and testing stresses. Similar results are recorded when cast steels of widely different tensile strengths are studied and the testing stress is expressed as a percentage of tensile strength. Less than 10 percent of the total cyclic life is spent in Stage II crack propagation for bending fatigue.

The effect of brittle inclusions increases the rate of crack propagation.

PREFACE

to the

RESEARCH REPORT

The studies of this report add to the information on the dynamic loading in fatigue of cast steels. The total information now available in SFSA Research Reports and found in the Steel Foundry Research Foundation Reports is given in the Steel Castings Handbook in summary form and in SFSA Engineering Data File reports.

Fatigue studies of cast steels and their presentation are most helpful for design engineers because for a large part, steel castings are employed in industry in dynamic loading operations. It is, therefore, most important for all steel foundrymen to make all the fatigue studies available to design engineers.

It is the policy of the Technical Research Committee and the SFSA research program over the past years to have continuing fatigue studies going forward.

The research on fatigue properties of cast steels have been carried on at Case Institute of Technology in its entirety and continuity in the studies have been established. The present research by Constantine Vishnevsky and J. F. Mang was undertaken in partial fulfillment for advanced degrees in the Department of Metallurgy, Case Institute of Technology. The Technical Research commends their excellent presentations and appreciates the guidance and assistance of Professor John Wallace.

CHARLES W. BRIGGS
Director of Research
Steel Foundry Research Foundation

April 1967

FATIGUE OF CAST STEELS

PART I-A STUDY OF THE NOTCH EFFECT AND OF THE SPECIMEN DESIGN AND LOADING ON THE FATIGUE PROPERTIES OF CAST STEEL

by

Constantine Vishnevsky and John F. Wallace

Graduate Assistant and Professor, Department of Metallurgy

Case Institute of Technology

PART II-FRACTOGRAPHIC STUDIES OF FATIGUE IN CAST STEEL

by

J. F. Mang and J. F. Wallace

Graduate Assistant and Professor, Department of Metallurgy

Case Institute of Technology

Steel Foundry Research Foundation

in contract with

Case Institute of Technology

PART I

A STUDY OF THE NOTCH EFFECT AND OF THE SPECIMEN DESIGN AND LOADING ON THE FATIGUE PROPERTIES OF CAST STEEL

SECTION 1. THE NOTCH EFFECT ON FATIGUE OF CAST STEEL

Introduction

The resistance of structures and parts to cyclic stresses is often of prime importance in the design of engineering structures. Increasing demand by engineers for more reliable performance information has produced a growing need for precise fatigue behavior data for engineering materials in general and metals in particular. Such information is needed for weight reduction of parts and cost reduction of structures so as to lessen the margins of error (Design Safety Factors).

Nearly all structures contain stress raisers of one type or another. For problems involving man-designed intentional notches such as fillets, keyways, and holes, extensive compilations exist on the theoretical increase in stress produced by different stress raisers under different loading conditions.^(1, 2) Such theoretical stress concentration factors tend to overestimate the fatigue strength reduction resulting from a notch. This has led to the concept of the notch sensitivity factor of a material in fatigue, q , relating the theoretical stress concentration factor, K_t , and the actual strength reduction factor, K_f , by $q (K_t - 1) = K_f - 1$.

The stress concentration factor, K_t , may be combined with a strength theory (distortion energy theory) to account for the biaxial nature of stress at the base of notches in certain stress states. Such a combination provides a more realistic prediction of strength reduction. This effective stress concentration factor, K_{te} , is recommended for large components.⁽³⁾

The value K_f tends to increase at a smaller rate than K_t or K_{te} for increasingly sharp notches. A linear relation is reported between K_t and K_f up to a critical value of K_t ; below this critical value of K_t , K_f will decrease indicating less strength reduction for very sharp notches compared to a slightly smaller severity.⁽⁴⁾ When this behavior is expressed in terms of q , increasing K_t leads to a decrease in the notch sensitivity factor.

Another type of variable affecting fatigue is the actual surface condition of the metal part. Highest stresses tend to appear at the surface and fatigue failures usually originate here. Reductions in fatigue life result from soft surface layers or surface residual tensile stresses and condition of the surface. The most desirable condition to obtain good fatigue properties is a polished surface, followed in order by ground (without introducing residual tensile stresses), machined and various degrees of cast surfaces, depending on the smoothness of the casting surfaces.

Fatigue investigations on cast steels comparing surfaces with different notch effects are few in number. One study compared notched and unnotched endurance ratios for normalized cast steels made by different steelmaking processes in the 75,000 to 95,000 psi tensile strength range. This work showed a slight superiority for acid electric and acid open-hearth steel in unnotched specimens and no essential differences for notched bar tests.⁽⁵⁾ An extensive comparison of cast and wrought steels of similar compositions and strength levels has shown that their notched endurance properties are very similar, but that the unnotched values are higher for wrought steels tested in the direction of rolling.⁽⁶⁾ These studies also pointed to the fact that cast steels are less notch sensitive than comparable wrought steels. Data on the effect of cast surfaces on the endurance limit were also presented since some cast surfaces can be likened to minor notch effects.

Additional information has been needed on the influence of machined notches on the fatigue properties of cast steel and it was for this purpose that the investigations of this research were undertaken.

Procedure

Composition . . . Several Ni-Cr-Mo cast steels (8630), fine grained, aluminum treated were employed in the studies. All were made under comparable conditions to similar analysis as listed in

Table 1. The steel was cast into sand molds to produce keel block coupons according to ASTM specification A-370. Tensile and R. R. Moore fatigue specimens were machined from the coupon legs after heat treating.

The steels were heat treated to two strength levels, 125,000 to 145,000 psi by water quenching and tempering and 80,000 to 90,000 psi by normalizing and tempering.

Test Specimens. . . The machined tensile specimens had a diameter of 0.357 inch in the 1.4-inch gage length. Three types of R. R. Moore fatigue specimens were used as illustrated in Figure 1. The surfaces of the unnotched specimens were ground and polished longitudinally in the test section with progressively finer abrasive papers until all traces of circumferential scratches were removed. The final polishing was done with fine emery.

Two different notches were studied for the notched specimens. Both types were 0.035 inch deep with a 60 degree included angle, but the radius at the bottom of the notch was different

with both the 0.015 and 0.001 inch radius being employed. The base of the 0.015 inch radius notch was polished, whereas the 0.001 inch radius notch was turned to size in a series of steps to assure accurate dimensions and was not polished. The final diameter of the notched specimens at the base of the notch was 0.220 inch or equal to the minimum diameter of the smooth bar specimen.

Mechanical Testing . . . Property values resulting from tensile and hardness testing are listed in Table 2.

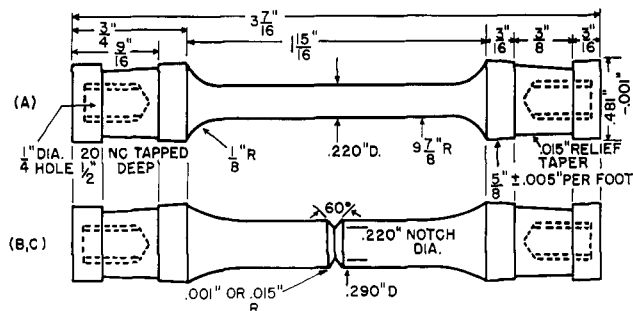


Figure 1—R. R. Moore type of fatigue specimens.

TABLE 1
Chemical Analysis of Ni-Cr-Mo (8630) Cast Steels
Percent

Heat No.	C	Mn	Si	Cr	Ni	Mo	P	S	Acid Soluble Al
1	0.33	0.84	0.31	0.45	0.55	0.25	0.018	0.030	...
3	0.32	0.83	0.32	0.45	0.50	0.20	0.23
5	0.30	0.79	0.29	0.36	0.40	0.15	0.014	0.030	...
6	0.34	0.90	0.28	0.54	0.70	0.25	0.07
7	0.25	0.62	0.25	0.46	0.40	0.15	0.023	0.029	0.09
9	0.32	0.58	0.26	0.48	0.51	0.10	0.038	0.033	...
10	0.31	0.64	0.26	0.45	0.50	0.25	0.025	0.025	...

TABLE 2
Tensile and Hardness Values for Ni-Cr-Mo (8630) Cast Steels of Table 1*

Heat No.	Heat Treatment	Tensile Strength psi	Yield Strength 0.2% psi	Red. Area %	Elong. %	BHN	Type of R. R Moore Specimen
1	NT	87,300	56,800	32.7	20.3	170	Unnotched
9	NT	88,900	49,300	33.8	19.6	173	**Notched 0.015
5	NT	83,400	52,300	37.5	22.2	167	Notched 0.001
7	NT	83,100	52,800	35.1	21.4	167	Unnotched
6	QT	145,000	128,000	32.9	12.1	321	Notched 0.015
3	QT	126,000	110,000	44.2	16.1	274	Unnotched
1	QT	132,000	117,000	28.4	11.4	285	Notched 0.015
10	NT	109,000	75,000	22.2	10.4	241	Unnotched
	QT	107,000	87,700	46.1	18.6	235	Notched 0.001
							Unnotched

* Average values for two tests, N - Normalized, NT - Normalized and Tempered, QT - Quenched and Tempered, ** Radius - inches.

Fatigue testing of the R. R. Moore specimens was carried on in four point reversed bending on standard R. R. Moore rotating beam machines at 10,000 rpm.

The fatigue tests were carried out at different stresses to obtain curves of stress versus cycles to failure. The number of specimens used for an S-N curve ranged from seven to eleven. The endurance limit was based on ten million cycles, so that specimens which did not fail after that number of stress reversals were considered to possess infinite life.

The Effect of Notches in Fatigue

The fatigue data for the Ni-Cr-Mo (8630) cast steel as unnotched and notched R. R. Moore specimens appear in the form of S-N curves, Figures

2, 3 and 4. The endurance strength limits and endurance ratios are summarized in Table 3.

It is observed from Table 3 that smooth bars, highly polished, record the highest endurance limits. A severe notch with a 0.015 inch radius at the bottom of the notch will result in the steel having much lower endurance limit, in fact a 36 percent reduction because of the presence of a serious notch. When the notch is made more severe, such as by reducing the radius of the bottom of the notch to 0.001 inch, the reduction of the endurance limit is greater, being 42 to 53 percent reduction.

The notch has a greater effect on the quenched and tempered steel than the normalized and tempered steel, with very severe notches exhibiting a reduction of 53 percent. The notch normally

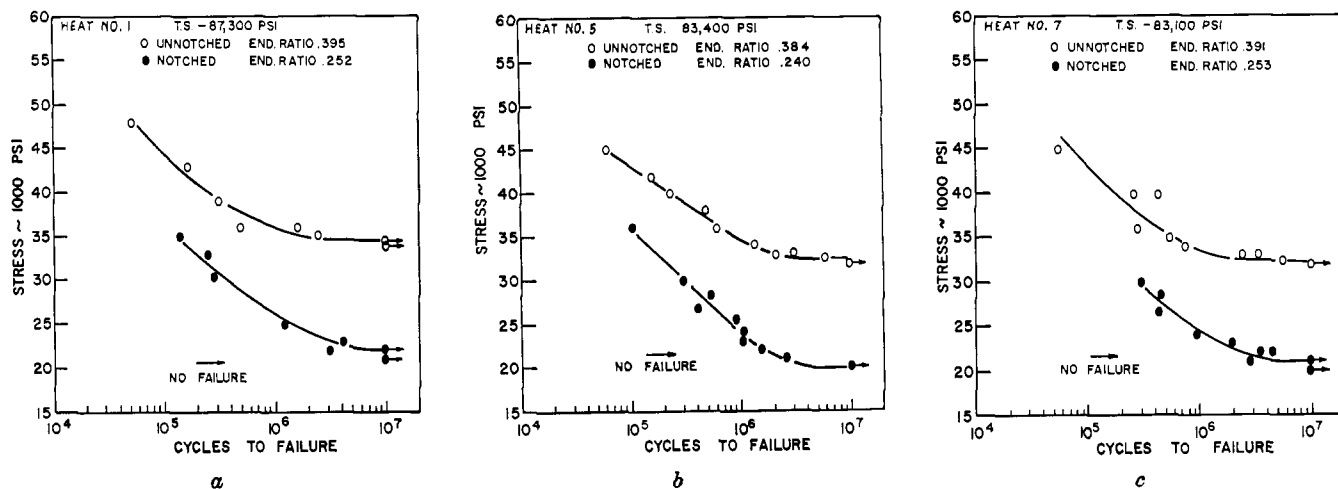


Figure 2—S-N curves for notched (0.015 inch radius) and unnotched R. R. Moore specimens. Normalized and tempered Ni-Cr-Mo (8630) cast steel.

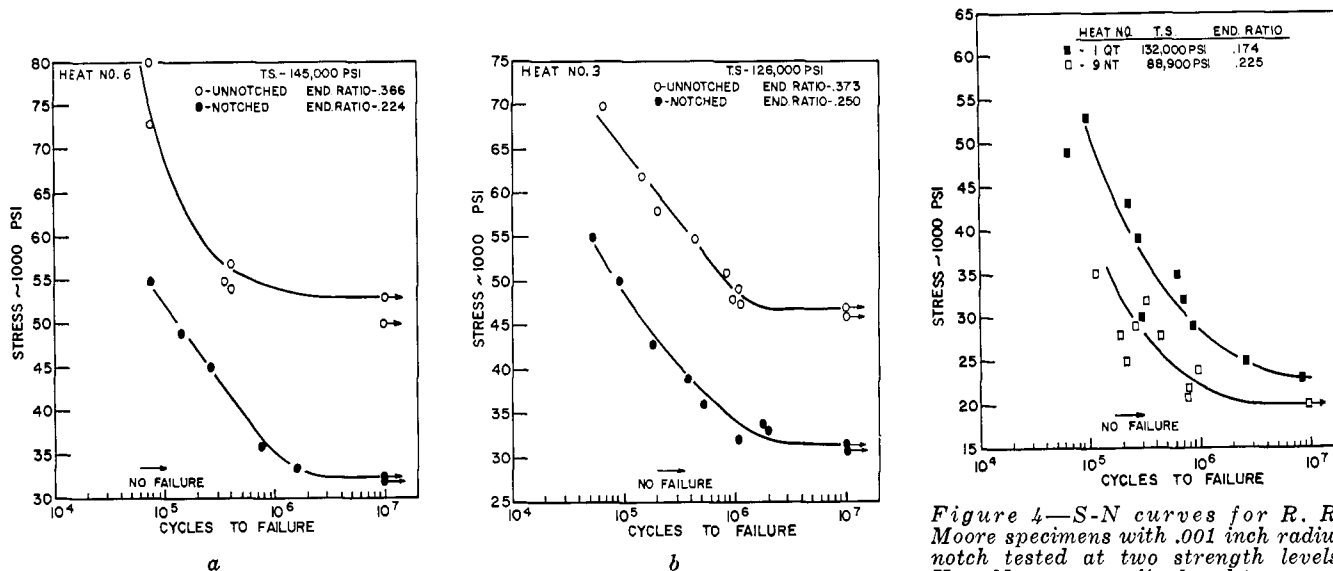


Figure 3—S-N curves for notched (.015 inch radius) and unnotched R. R. Moore specimens. Quenched and tempered Ni-Cr-Mo (8630) cast steel.

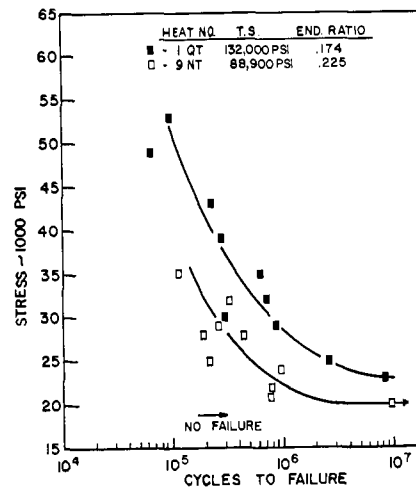


Figure 4—S-N curves for R. R. Moore specimens with .001 inch radius notch tested at two strength levels. Heat No. 9 - normalized and tempered. Heat No. 1 - quenched and tempered Ni-Cr-Mo (8630) cast steel.

TABLE 3
Summary of Fatigue Results for R. R. Moore Tests of Ni-Cr-Mo (8630) Cast Steels

Heat No.	Heat Treatment	Tensile Strength psi	No Notch	Endurance Limit psi Notched in.-R		No Notch	Endurance Ratio* Notched in.-R	
				0.015	0.001		0.015	0.001
1	NT	87,300	34,500	22,000		0.395	0.252	
9	NT	88,900	20,000			0.225
5	NT	83,400	32,500	20,000		0.384	0.240	
7	NT	83,100	32,500	21,000		0.391	0.253	
						Avg. 0.390	0.248	0.225
6	QT	145,000	53,000	32,500		0.366	0.224	
3	QT	126,000	47,000	31,500		0.373	0.250	
1	QT	132,000	23,000			0.174
						Avg. 0.370	0.237	0.174

NT - Normalize and Temper, QT - Quench and Temper, R - Radius at bottom of notch in inches, * - Endurance Limit/Tensile Strength.

employed in fatigue testing of 0.015 inch radius at the bottom of the notch resulted in a 36 percent reduction irrespective of heat treatment.

It is interesting to note that the endurance ratio for both notched and unnotched test values is at a higher level for normalized and tempered cast steel than for the same steel in the quenched and tempered condition.

Values have been calculated for the stress concentration factor K_t , the fatigue strength reduction factor K_f and the notch sensitivity factor q for the fatigue test results and these values are presented in Table 4. The K_t value of 2.2 represents a severe notch. In comparison most steel casting fillets are designed to have K_t values less than 1.4 in tension or bending. A notch having a K_t value of 6.2 is an extreme condition and would lower the endurance limit to nearly its lowest value.

Table 4 shows that the highest values of K_t were obtained for the sharper notches, as was to be expected. A K_t value of 2.12 for the higher strength quenched cast steel is compared to the 1.73 of the normalized cast steel. The higher the number the greater is the fatigue strength reduction. Thus when very severe notches are employed, the notch is more effective in reducing the fatigue strength of the higher strength cast steel than steels of lower strength.

The severe notch of 0.015 inch radius ($K_t=2.2$) does not show similar fatigue strength reductions since the quenched steel values range from 1.49 to 1.63 while similar values of 1.54 to 1.61 are recorded for the normalized cast steel.

The notch sensitivity factor, q , defined as $q(K_t - 1) = K_f - 1$ was calculated using a K_t of 2.2 for

TABLE 4
Fatigue Strength Reduction and Notch Sensitivity Factors for R. R. Moore Specimens Ni-Cr-Mo Cast Steel

Notch Radius in.	Tensile Strength psi	$K_t^{(1)}$	$K_f^{(2)}$	$q^{(3)}$
0.015	87,300	2.2	1.57	0.475
0.015	83,400	2.2	1.61	0.509
0.015	83,100	2.2	1.53	0.450
0.015	145,000	2.2	1.63	0.525
0.015	126,000	2.2	1.49	0.408
0.001	132,000	6.2	2.12	0.216
0.001	88,900	6.2	1.73	0.140

- (1) Theoretical stress concentration factor
- (2) Fatigue strength reduction factor = endurance limit for unnotched specimens / endurance limit of notched specimens
- (3) Notch sensitivity factor, $q = (K_f - 1) / (K_t - 1)$

the 0.015 inch radius notch and 6.2 for the 0.001 inch radius notch. The factor q is lower for the sharper, 0.001 inch radius, notches than for the 0.015 inch radius notches. This is in agreement with the usual behavior observed in fatigue testing. The factor q was 0.216 for the quenched and tempered condition and for annealed specimens it was 0.140. These values are also in agreement with the general tendency for lower strength steels to be less notch sensitive than those that are quenched and tempered⁽⁷⁾.

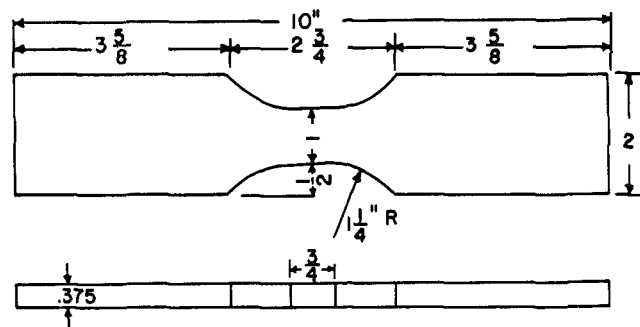
The notch sensitivity factor, q , varied from 0.408 to 0.525 for tests with 0.015 inch radius notches and did not vary to any degree with tensile strength. A few tests on cast 8630 steel⁽⁶⁾ using the same specimen types and notch (0.015 inch radius) as those of the present study obtained values for q of 0.57 for the quenched and tempered condition (T.S. 137,500 psi) and 0.53 for the normalized and tempered condition (T.S. 110,500 psi),

SECTION 2. THE EFFECT OF SPECIMEN DESIGN AND TYPE OF LOADING ON THE FATIGUE OF CAST STEEL.

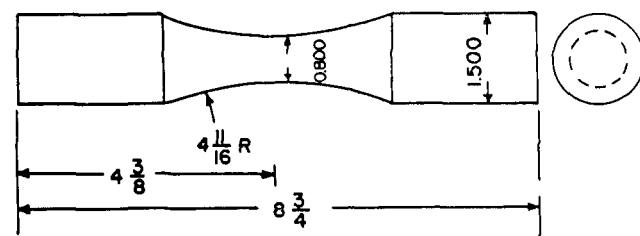
Introduction

It is generally recognized that the common practice of performing fatigue tests on small rotating beam fatigue specimens, such as the R. R. Moore specimens, is of value in elucidating differences between materials—the applicability of these data to engineering components must be done carefully. Also it is known that the size of the test specimen and its shape affects fatigue results to the extent that a lower endurance strength is obtained for larger specimens. (8) The size effect is also observed in cyclic torsion. (9) Naturally it is desirable to perform fatigue tests on whole structures but the obvious cost considerations and test equipment availability often make such testing impossible.

Fatigue studies have been made employing different design of test specimens and size of the specimens when compared to the R. R. Moore specimens of Figure 1. The design and size of the specimens employed other than those of the R. R. Moore specimen design are shown in Figure 5. The application of the loads for these specimens is different from that for the R. R. Moore specimens.



a) PLATE BENDING FATIGUE SPECIMEN



b) TORSION FATIGUE SPECIMEN

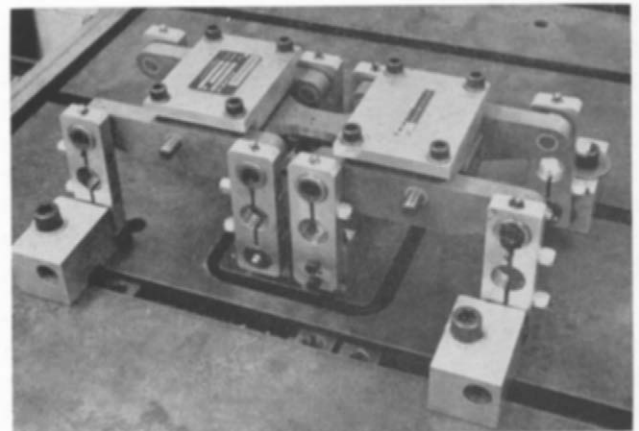
Figure 5—Bending and torsion fatigue specimens.

Procedures

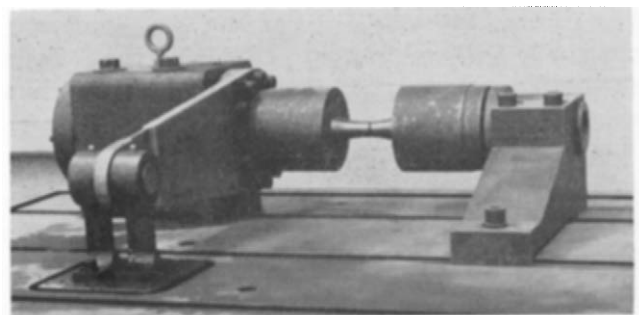
The plate bending and bar torsion fatigue specimens were cast three to a mold using a gating and riser technique that would produce radiographically sound steel castings from cast steels listed in Table 1.

The plate bending fatigue specimens were machined from the one-half inch thick cast steel plates. The torsion bars were ground on a rotary surface grinder to a diameter of 0.800 inch. Surface finish of the test section was 20 microinches.

Mechanical Testing . . . Property values resulting from tensile testing are listed in Table 2. The plate bending and torsion fatigue tests were conducted on a constant load amplitude Sonntag SF-1-U fatigue machine at 1800 cycles per minute. The plates were tested in reversed bending under four-point loading in the fixture shown in Figure 6a. The torsion test set-up is shown in Figure 6b. A lever arm connected to the vibrating platen transmitted the torque to collets gripping the torsion specimen.



a. Plate specimen tested in reverse bending fatigue.



b. Bar specimen tested in torsion fatigue.

Figure 6—Fixtures for the Sonntag fatigue machine.

Fatigue specimens were considered as failed when the machines were shut off by amplitude limiting switches. This amplitude limit corresponded to fracture of the entire test section for all bending fatigue tests. The torsion tests were terminated by the switches because of the deflection limitations of the fatigue machine. In all but one case, this deflection limitation was attained after the specimen had been severely cracked. The endurance limit was based on ten million cycles.

Plate Bending Fatigue Tests

The S-N curves obtained for all reversed bending fatigue tests of cast steel plate specimens are located in Figure 7. These curves provide a qualitative comparison between fatigue results because of the variations in tensile strength for similar heat treatments. A more exact evaluation of various variables may be obtained by examining the endurance ratios.

The endurance ratios for the normalized and tempered, and quenched and tempered heat treatments of specimens from cast steel plates tested in reverse bending were 0.360 and 0.310, respectively, and are lower than the average values obtained for unnotched R. R. Moore specimens. Such a difference between the two types of tests is not surprising. The casting methods and solidification process were very different with the keel block having 3 cooling faces, controlled directionally solidified toward the riser, whereas the plate consists of 2 cooling faces of uniform section thickness. Also the specimens were geometrically dissimilar and the lower endurance ratio obtained for the larger plate specimens is consistent with the size effect.⁽⁸⁾

The type of fatigue test and speed of testing must also be considered in comparing rotating beam and cantilever fatigue results: for example, (4130) a Cr-Mo steel of tensile strength of 150,000 psi tested at a 15 percent reduction in fatigue strength for cantilever specimens as compared to R. R. Moore tests.⁽¹⁰⁾ Another study more applicable to the present research compared Sonntag and R. R. Moore machines.⁽¹²⁾ The R. R. Moore machine and specimens were tested at 10,000 and 1800 rpm; R. R. Moore specimens were tested in reversed plane bending on a Sonntag machine at 1800 cycles per minute; and plates of the same thickness as the minimum diameter of the R. R. Moore specimens (0.300 inch) were also studied in reversed bending on a Sonntag machine at 1800 cycles per minute. These fatigue tests of a Ni-Cr-Mo (4340) steel (T.S. 127,000 psi)

showed that rotating beam tests were more severe than the plane bending of round specimens. Also rotating bending is more severe than plane bending of plates. The results of this study and of other tests⁽¹²⁾ proved that an increase takes place in the endurance limit at the higher speeds of testing.

Evidently, the exact factors contributing to the lower fatigue performance of the sound plate castings are complex because of the solidification characteristics and are not fully resolvable.

The endurance limits and endurance ratios for all plate bending tests are listed in Table 5. It must be appreciated, however, that the endurance ratio of the sound (unnotched) plate bending specimens is lower than the ratio for unnotched R. R. Moore specimens.

Torsion Fatigue Tests

The fatigue results for reversed torsion tests are presented in the form of S-N curves in Figure 8. The endurance ratios are listed in Table 5.

The endurance ratios were higher for the higher strength steel. This is in contradiction with the effect of tensile strength noted for R. R. Moore specimens and in the sound plate specimens.

Comparison of Torsion and Bending Fatigue Results

Either the maximum shear stress or distortion energy theory can be used in comparing torsion

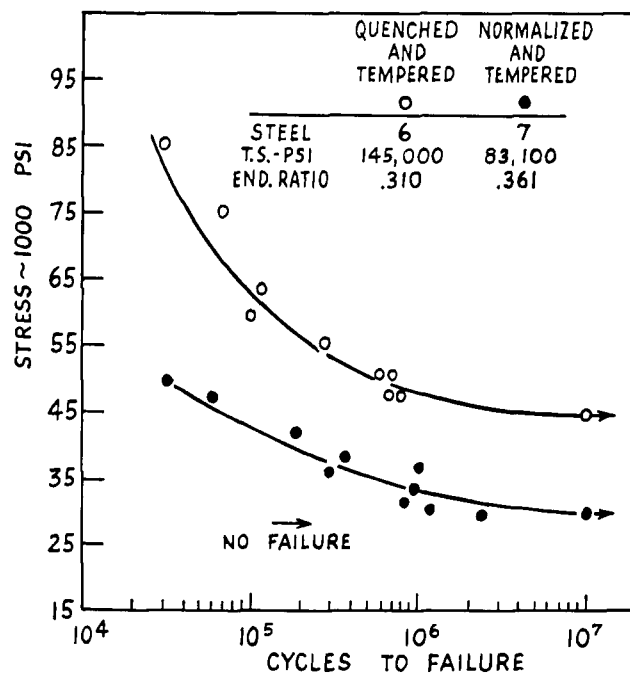


Figure 7—S-N curves for Ni-Cr-Mo (8630) cast steel tested as plate specimens, in reversed bending at two strength levels.

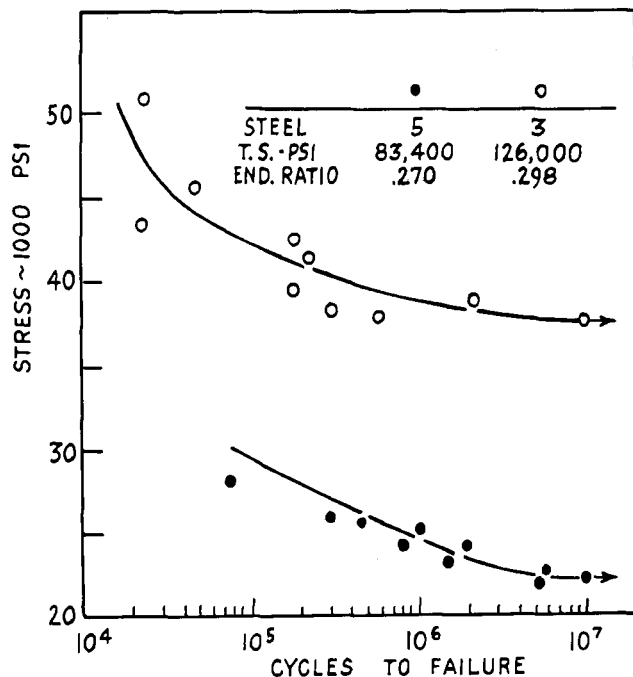


Figure 8—S-N curves for Ni-Cr-Mo (8630) cast steel tested as bar specimens in torsion at two strength levels.

TABLE 5

Comparison of Torsional Endurance Ratios Corrected by Two Strength Theories with Endurance Ratios Measured in Bending

		Heat Treatment	
		NT	QT
Torsion (measured)	A	0.270	0.298
Torsion (corrected)	B ⁽¹⁾	0.540	0.596
	C ⁽²⁾	0.468	0.516
Plate Bending		0.361	0.310
R. R. Moore Avg.		0.390	0.369

- (1) Maximum shear stress theory: B=2A
 (2) Distortion energy theory: C=1.73A

and bending fatigue results for cast steels. The maximum shear stress theory predicts that the ratio of endurance limit in torsion to that in bending will be 0.5 and the distortion energy theory predicts a ratio 0.577. These laws are well obeyed for ductile metals.⁽¹³⁾

The corrected values of endurance ratio for the torsion tests using each theory together with some of the endurance ratios obtained in plane and rotary bending are listed in Table 6. The corrected endurance ratios for torsion are considerably higher for similar strength levels than the measured values in bending. Even the agreement between R. R. Moore specimens and the corrected endurance ratios for torsion specimens is poor. This is surprising since the R. R. Moore specimens were machined from cast steel keel blocks and

should exhibit the more consistent properties from the standpoint of the solidification process.

A parallel approach for comparing these results is to examine the ratio of endurance limit in bending to the uncorrected endurance limit in torsion. This ratio is referred to in the literature as either f_o/q_o or b/t . The distortion energy and maximum shear stress theories predict b/t ratios of 1.73 and 2.00, respectively. Table 6 lists b/t computed using results of unnotched R. R. Moore specimens and plates with and without slag. Since in some cases the tensile strengths of the lots compared at similar heat treated conditions differed slightly, b/t was calculated by dividing the endurance ratio in bending by the endurance ratio in torsion, similarly to the method used for strength reduction factors. Table 6 shows that at lower tensile strength levels, b/t is closer to the theoretical values of 1.73 and 2.00 but that for quenched and tempered material the deviation from theory is large.

Some previous work on wrought steels and cast irons studied the variation of b/t in the presence of stress raisers. A b/t ratio value of 1.57 for unnotched 4340 steel and 1.68 for notched tests was obtained. Another study⁽¹⁵⁾ on seven steels showed the following average ratios: unnotched-1.66, notched-1.29, drilled-1.39. Measurements on four cast irons, a metal which contains many inherent notches, computed an average ratio of slightly less than one ($b/t = 0.961$).

The results obtained in the present work on cast steel when viewed in the light of the above data suggest that notch effects in cast steels, such as designed-in notches or discontinuities, are less damaging in torsion than in bending,

Decarburization

It is well-known that fatigue properties are reduced by decarburized layers such as could occur at stress concentration points because of location of surface discontinuities and improper heat treating operations. One investigation⁽²³⁾ was made on

TABLE 6

Values of b/t Ratio Comparing Bending and Torsion Fatigue Results

Heat Treatment	b/t (1)	
	(2)	(3)
NT	1.34	1.44
QT	1.04	1.24

- (1) Endurance ratio in bending/endurance ratio in torsion
 (2) b from plate casting tests
 (3) b from R. R. Moore tests

the effect of decarburization of a steel of different microstructures on the nucleation and propagation of fatigue cracks. The studies revealed that the order of first crack formation was pearlite, then tempered martensite and lastly, martensite. However, crack propagation rates were relatively slow in tempered martensite and pearlite but fast in martensite. The reductions in the endurance limit of unnotched specimens for various structures were as follows : martensite-50 percent, tempered martensite-40 percent, pearlite-30 percent. Depth of decarburization was not found to exert a significant role on fatigue strength reduction.

The effect of decarburization in both notched and unnotched specimens has been examined for

some alloy steels.⁽¹⁶⁾ These studies showed that the major influence on fatigue strength is the hardness of the decarburized skin, and that decarburization lowers the fatigue curve by a smaller amount for notched than unnotched specimens.

Neither the extent of decarburization nor the influence of stress raisers and microstructure in the present study could be readily established. However, it was advisable to comment on the possibilities of the problem in view of the fact that steel castings are employed in bending and torsion fatigue service in the unmachined condition after heat treatments that sometimes are rather long at high temperatures under conditions of maximum decarburization of casting surfaces.

CONCLUSIONS TO PART I OF THE RESEARCH REPORT

The following are the conclusions suggested by the results of these studies :

1. A severe notch with a 0.015 inch radius at the bottom of the notch in a fatigue test specimen (R. R. Moore) will result in a cast steel having a low endurance limit. The severe notch results in a 36 percent reduction when compared to fatigue test on bars with no notches. Any extremely severe notch (bottom radius 0.001 inch) results in a 42 to 53 percent reduction of the endurance limit.

2. No consistent or large effect of heat treatment is observed on the reduction of fatigue strength of cast steel for 0.015 inch radius notched R. R. Moore specimens. However, for the more severely notched specimens, 0.001 inch radius notch, the fatigue strength reduction factor, K_f , is appreciably higher for cast steel in the quenched and tempered condition.

3. A K_t (stress concentration factor) value of 2.2 represents a severe notch in cast steel. Most steel casting fillets are designed to have K_t values less than 1.4. A notch of K_t 6.2 is an extreme condition and would lower the endurance limit about 50 percent which would be about its lowest value for cast steel.

4. The lower strength cast steels (normalized and tempered) are less notch sensitive (factor q) than the higher strength cast steels (quenched and tempered).

5. Cast steel exhibits considerably better endurance properties in reversed torsion than reversed bending. The comparison is made by converting the torsional endurance ratios into equivalent values for reversed bending using either the maximum shear stress or distortion energy theory.

6. The relative fatigue behavior of cast steel in bending and torsion, as measured by the b/t ratio, deviates less from the theory for cast steels at the lower tensile strength level.

7. The endurance ratios for both unnotched R. R. Moore and cast plate bending fatigue tests are higher at the lower tensile strength level.

8. Bending fatigue tests of cast steel plates tested at 1800 rpm give lower endurance properties than rotating beam tests at 10,000 rpm. The difference is greater at the higher tensile strength level.

REFERENCES TO PART I

1. Peterson, R. E., Stress Concentration Design Factors, John Wiley, New York, 1953.
2. Lipson, C., and Juvinal, R. C., Handbook of Stress and Strength, Macmillan, New York, 1963.
3. Timoshenko, S., "Stress Concentration and Fatigue Failures," Proc. Inst. Mech. Engrs., Vol. 157, 1947, p. 163.
4. Frost, N. E., "Non-Propagating Cracks in Vee-Notched Specimens Subject to Fatigue Loading," Aero. Quarterly, Vol. 8, Feb. 1957, p. 1.
5. Sims, C. E., and Dahle, F. B., "Comparative Quality of Converter Cast Steel," Trans. ASTM, Vol. 42, 1942, p. 532.
6. Evans, E. B., Ebert, L. J., and Briggs, C. W., "Fatigue Properties of Comparable Cast and Wrought Steels," Proc. ASTM, Vol. 56, 1956, p. 979.
7. Lipson and Juvinal, p. 117.
8. Morkovin, D., and Moore, M. F., "Third Progress Report on the Effect of Size of Specimen on Fatigue Strength of Three Types of Steel," Proc. ASTM, Vol. 44, 1944, p. 137.
9. Lessels, J. M., Strength and Resistance of Metals, John Wiley, New York, 1954, p. 212.
10. Fuller, F. B., and Oberg, T. T., "Fatigue Characteristics of Rotating Beam Versus Rectangular Cantilever Specimens of Steel and Aluminum Alloys," Proc. ASTM, Vol. 47, 1947, p. 665.
11. Roos, P. K., Lemmon, D. C., and Ransom, J. T., "Influence of Type of Machine, Range of Speed, and Specimen Shape on Fatigue Tests Data," ASTM, Bul. No. 158, May 1949, p. 63.
12. Lessels, p. 205.
13. Lessels, p. 181.
14. Findley, W. N., Mergen, F. C., and Rosenberg, A. H., "The Effect of Range of Stress on Fatigue Strength of Notched and Unnotched SAE 4340 Steel in Bending and Torsion," Proc. ASTM, Vol. 53, 1953, p. 768.
15. Thurston, R. C. A., and Field, J. E., "The Fatigue Strength Under Bending, Torsional and Combined Stresses of Steel Test Pieces with Stress Concentrations," Proc. Inst. Mech. Engrs., Vol. 168, No. 31, 1954, p. 785.
16. Jackson, L. R., and Pochapsky, T. E., "The Effect of Composition on the Fatigue Strength of Decarburized Steel," Trans. ASM, Vol. 39, 1947, p. 45.

PART II

FRACTOGRAPHIC STUDIES OF FATIGUE IN CAST STEEL

Introduction

Failure of metals by fatigue results from repeated loads whose maximum can be much less than the static breaking load. Also, the greatest number of service failures occurs by dynamic rather than static loading. Much information on the characteristics of fatigue failure, its mechanism, origin, direction, and rate can be obtained from a macroscopic and microscopic analysis of the fractured surfaces.

Post fracture analysis of specimens that have fractured in fatigue has been limited to details of the fracture surface which could be resolved with the naked eye or low power magnifiers. Examination at higher magnifications was severely limited because of the short depth of field of focus of conventional light microscopes. Nevertheless, many important discoveries resulted from studies of this kind.

The most striking feature of the fatigue fracture surface on a macroscopic scale is its apparent lack of plastic deformation, even in very ductile metals. Small ridges, or "beach marks," caused by variations in the cyclic loading, are sometimes found on the fracture surface. The shape and dimensions of these marks provide important evidence on the point of crack initiation, type of loading, and the notch sensitivity of the material. The appearance of the area of final failure and the occurrence of "ratchet marks" indicate the stress level involved and the number of crack origins. Much other information about the failure and its causes can be surmised from the appearance of the fracture surface. ⁽¹⁻⁴⁾

The metallurgical microscope has been used extensively to study fatigue failure specimens and although it is possible to obtain magnifications up to 2000 X, its use is restricted to very smooth fracture surfaces by the short depth of field. The presence of fatigue striations and "platies," or areas believed bounded by grain boundaries and covered by fatigue striations, were first recognized with the metallurgical microscope. ^(5, 6)

Fracture surface analysis received considerable impetus after 1955 from the application of the electron microscope⁽⁷⁻⁹⁾ which permits magnifications of 200,000 X with good resolving power.

Fractography . . . The electron microscope cannot investigate the fracture surface directly by transmission. A replica of this surface may be produced from a less electron dense material. The principle of the replica technique is to transfer the topography of the fracture surface to a thin film. This film is then observed in the electron microscope. The most frequently used material for replicas is carbon. One method of producing a replica is by making a plastic negative of the fracture surface and then evaporating a 100 to 200 angstrom thick layer of carbon onto the negative in a vacuum. The plastic backing is then dissolved and the resulting replica is observed directly in the electron microscope. The contrast produced by replicas is often very low and it may be necessary to increase it by the technique of shadow casting. This consists of evaporating a thin film of electron dense material obliquely onto the negative surface.

The shadow casting technique on replicas is known as Fractography. The resolution obtained with replicas depends on the shadowing material used and varies from 50 to 100 angstroms. Magnifications from 1,000 X to 15,000 X have been found best for electron fractography.

Striated Fracture. . . The most important feature of a fatigue fracture surface is its lamellar or striated appearance. These striations are sometimes identifiable by the metallurgical microscope at high stress levels but are usually seen only with the electron microscope. Striations have been observed on the fracture surfaces of many materials, including mild steels, aluminum and its alloys, titanium and its alloys, stainless steel, polycarbonate resins and many others.

The lamellar or striated appearance of fatigue fracture surfaces has been explained in a number of ways. These include: a relationship to the cellular theory of metals;⁽⁵⁾ and a connection with

the cyclic loads. It was suggested that one striation may be equal to one load cycle.⁽⁷⁾ This equality was proved by examination of a programmed test load specimen⁽¹¹⁾ and corroborated by several investigators.⁽¹²⁻¹⁴⁾ These simple but important experiments showed not only that a striation is associated with each load cycle but that the size of the striation was a function of the applied stress. It was also found that the striation spacing increased with increasing crack length. Since the striation spacings are directly related to applied stress and crack length, it is apparent that post-fracture analysis of fatigue striations can provide valuable evidence as to the stress conditions associated with the failure.

Crack Propagation. . . Crack growth has been described as a two-stage process.⁽¹⁵⁾ Stage I is described as a slip plane cracking in those planes most closely aligned with the maximum shear stress direction. The actual mechanism of nucleation is believed to involve slip plane fractures caused by repetitive reversals of the operative slip systems which can form a slip band groove or "intrusion" and finally a crack. Mechanisms involving extrusions have also been proposed.⁽¹⁶⁾ For alloys of commercial purity, inclusions have been shown to be a location for the initiation of Stage I.⁽¹⁷⁾ Stage I can account for an appreciable portion of the life of the specimen. Small axially strained cycled specimens have been shown to have a large percentage of the cyclic life spent in Stage I for total lives over 10^4 cycles.⁽¹³⁾ No particular fractographic features exist in this stage.

In Stage II the crack propagates perpendicularly to the direction of maximum tensile stress by the mechanism of striation formation. This stage has been called the technical origin of the fatigue crack, since this is when the crack can be found by normal methods. Stage III is the final failure stage and occurs when the remaining cross section is too small to bear the applied load and failure results within a few cycles.

More than one theory has been proposed for the mechanism of striation formation, as discussed for Stage II above. According to some sources, a zone of heavy plastic deformation occurs ahead of the root of the crack. A void is formed in a brittle manner ahead of the crack tip because the volume is constrained from the hydrostatic tensile stresses in this area. Other investigators⁽¹⁸⁾ describe this as an increase in stress due to an accumulation of work hardening in the vicinity of the tip of the crack that exceeds the strength at this location. The original crack then advances into an area which has not been fully work hard-

ened and then stops. Other theories⁽¹⁹⁾ propose the formation of "ears" at the tip of the fatigue crack resulting from complex plastic deformation. This mechanism produces a cross section in which the ears or troughs mate to each other on the matching fracture surfaces. Still other workers⁽²⁰⁻²¹⁾ believe that striation formation can be fully explained by crack propagation on the existing crystallographic planes.

Although little agreement exists among investigators on the mechanism of striation formation, the occurrence of Stage I and Stage II is well accepted. Stage I, while being always important in pure metals, sometimes does not apply in commercial metals because of the presence of notched shaped discontinuities, scratches, metallurgical notches, production defects, machined-in notches and notches relating to the design of the part. These types of discontinuities may initiate Stage II crack propagation immediately under certain stress conditions.

Procedure and Materials

Fatigue Specimens. . . The R. R. Moore fatigue specimens were produced from cast Ni-Cr-Mo (8630) steel of compositions listed in Table 1, (part I of this report).

The steel was cast in sand molds as keel blocks according to ASTM specifications A370-54T.

The cast steel was aluminum deoxidized to produce a small austenitic grain size and was heat treated to produce two structures and strengths. Quenching and tempering obtained tensile strengths of 105,000 to 145,000 psi with a tempered martensite structure and normalizing and tempering gave strengths of 80,000 to 110,000 psi with a ferritic-pearlitic structure.

After heat treatment, the coupon legs from the keel blocks were machined into tensile and fatigue specimens. The tensile specimens were standard with a diameter of 0.357 inch in the 1.4-inch gage length. Two types (unnotched and notched) of R. R. Moore specimens were employed as illustrated in Figure 1 of Part I. The surfaces of the unnotched specimens were ground and polished. The notched specimens had a 0.035-inch deep notch with a 60 degree included angle and a 0.015-inch notch radius. The base of the notch was polished. The final diameter of the notched specimens at the base of the notch was 0.220 inch or equal to the minimum diameter of the smooth bar specimens.

Tensile test properties of the Ni-Cr-Mo cast steel are given in Table 2, Part I.

The fatigue testing was conducted on standard R. R. Moore rotating beam machines at 10,000 rpm. The specimens tested during the initial stages were loaded at various stresses to determine the S-N curves for the two microstructures at the various strength levels. Additional tests of both the tempered martensite and ferritic-pearlitic structures were conducted for the steel of equal strength levels at four testing stresses to determine the relative rates of crack propagation over a wide range of life to failure.

Unfortunately, the R. R. Moore testing machines did not stop rotating quickly enough after failure of the specimens in some cases to prevent damage to the fracture surfaces by bumping together. These damaged specimens were removed from the group from which useful information was obtained. Another source of discarded specimens was abnormal fractures, such as an unnotched specimen whose crack was initiated at two widely separated points.

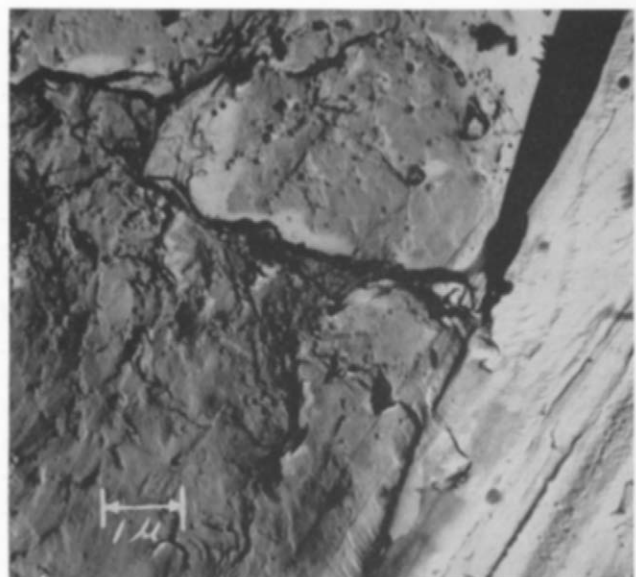
The preparation of the replicas is given in Appendix I.

Crack Initiation

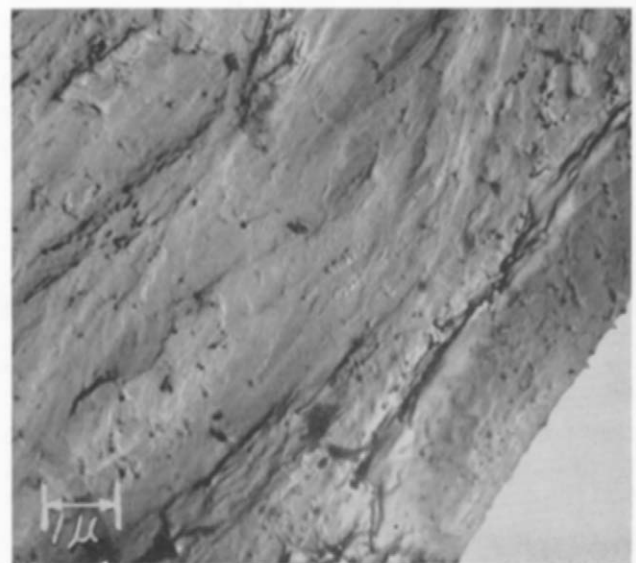
Replicas of the crack initiation site and surrounding areas were investigated for the fatigue fracture surfaces of twelve unnotched and notched R. R. Moore specimens in both the normalized and quenched and tempered condition. These replicas exhibited a somewhat "rubbed" or "ground" appearance with a minimum of surface detail. Fatigue striations were not found in the immediate vicinity of the apparent crack initiation sites. Other investigators have encountered this same condition. It is caused by rubbing together of the fracture surfaces or to a shear mechanism operating in Stage I. The very edge of the specimen, where the crack probably was initiated, is the area where the most damage occurred.

In spite of these difficulties, many discontinuities were found in the fractographs in the area of the apparent crack initiation sites. Figure 9a shows a jagged crack entering the main crack surface. Note the rubbed appearance of the surface in this fractograph and in 9b. A crack, shown in Figure 9b intersects the main crack surface parallel to the edge of this quenched and tempered specimen. No apparent difference in the fractographic appearance of Stage I was noted for the two microstructures investigated.

Crack initiation takes place on planes other than those of Stage II crack propagation since Stage I occurs on slip planes closely aligned with the crit-



a. Normalized and tempered, notched specimen.



b. Quenched and tempered, unnotched specimen.

Figure 9—Fractographs of discontinuities found at the apparent crack initiation site.

ically resolved shear stress. The Stage II crack propagation planes are perpendicular to the tensile direction and are the planes of the fractographs shown. It is reported⁽²⁴⁾ that a cleavage crack perpendicular to the direction of applied stress forms first in Stage II and that striations develop subsequently. The discontinuities found may well be involved with crack initiation but the damaged surfaces in these areas prevent complete identification.

Stage I to Stage II Transition

The rubbed appearance found at the site of crack initiation extended in the direction of crack propagation for variable distances, depending

upon the degree of damage to the fracture surface. Patches of fatigue striations are encountered with adjacent areas of rubbed surfaces, as shown in Figure 10, further into the specimen toward the final failure area. The striation bearing surfaces appear to lie on somewhat divergent planes from that of the damaged surfaces. Well defined striations appeared as close as 0.005 inch from the edge of the specimen but in the case of heavy damage were sometimes not clearly visible until 0.015 inch into the specimen. Specimens tested at low stress, where a larger number of cycles were recorded in Stage II crack propagation, exhibited the most damage. Further into the specimen in the direction of crack propagation, fatigue striations are observed covering the surface of the specimen.

The transition from Stage I to Stage II is a subject that has not been fully explained. Most investigators agree that Stage I occupies only a very small percentage of the crack length. Well defined striations have been found at 0.005 inch of crack depth in most of the specimens investigated and it is possible that striations did exist prior to this distance but were obliterated by the rubbing of the fracture surfaces. The patches of striations found on a slightly divergent plane were protected from rubbing damage by higher spots at the edges where the plane diverges from the dominant crack surface. As the depth increases, rubbing damage decreases but does not entirely disappear as shown in Figure 11. The fractograph of Figure 11, taken 0.025 inch from the crack initiation site, still shows the effects of light surface rubbing. Some of the higher areas in this

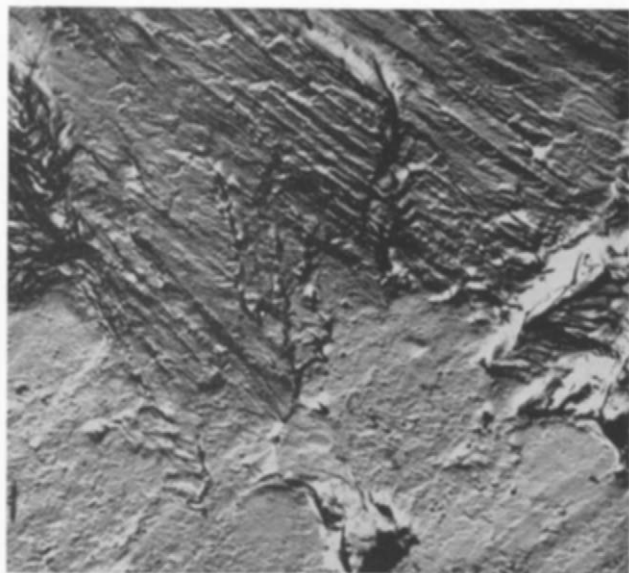


Figure 10—Fractographs of Stage I to Stage II transition areas.

fractograph have had their surfaces rubbed until they contain no features. The extent of rubbing damage can be macroscopically estimated from the depth of the surface that appears to be very shiny. The direction of crack propagation is indicated in the fractographs by an arrow.

Surface Morphology Versus Microstructure

Stage II, or the crack propagation stage of fatigue failure, was investigated by studying the same replicas used for crack initiation as well as cross sections through the fracture surface. Areas of well defined striations were found accompanied by areas of ill defined striations and ruffled areas showing no striations.

Typical fractographic appearances for cast steel with a pearlite plus ferrite microstructure are shown in Figure 12. A large percentage of the surface covered with striations is observed in Figure 12. Areas of poorly defined striations and some featureless areas are also in evidence. The dark lines separating areas of striations have been termed "tear ridges" and connect areas of different elevation. The fractographic appearance of the cast pearlite plus ferrite structure is similar to those of mild wrought steels reported in the litera-

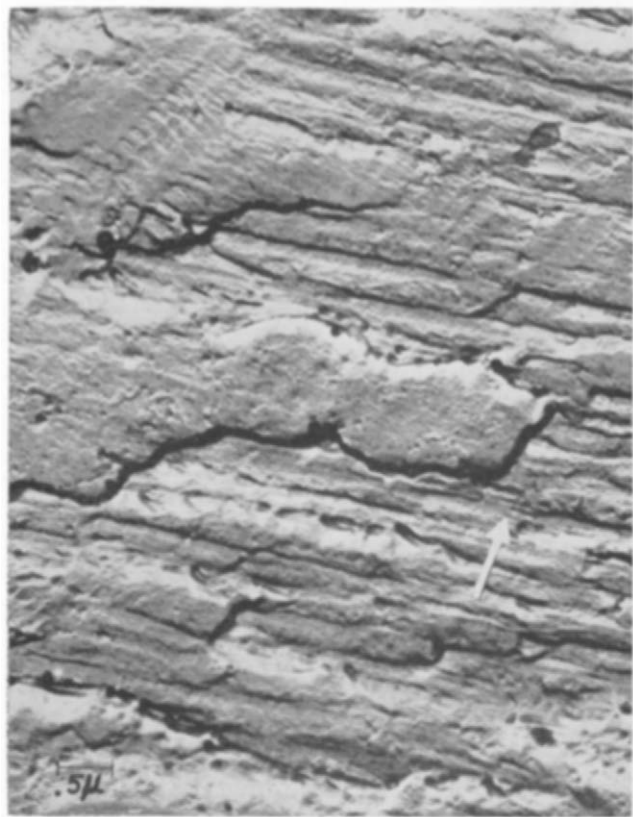


Figure 11—Fractograph of fatigue striations at .025 inch from the crack initiation site showing the effect of rubbing damage. Direction of crack propagation is identified by arrow.

ture, although the cast steel exhibits more well defined striations than those of wrought steels.

Replicas of polished and etched cross sections through the fracture surface disclosed well defined striations in the ferrite portions of the crack surface. Figure 13 shows cross sections of brittle and ductile appearing striations in ferrite.

An area of pearlite at the fracture surface is illustrated in Figure 14a. The cementite plates form ductile striction shaped mounds on the fracture surface which could be mistaken for striations but are in most cases too large for the spacing anticipated. Figure 14b shows adjacent ferrite and pearlite regions at the fracture surface. In some cases, striations appear to be super-imposed on the cementite plates.

The fractographic appearance of quenched and tempered cast steel is shown in Figure 15. The striations in this material are sometimes indistinct and not recognizable. However, an area of fairly well defined striations is shown in Figure 15. This type of surface morphology is similar to wrought high strength steels reported in the literature. Replicas of cross sections through martensitic fracture surfaces, as shown in Figure 16, generally displayed irregular striations.

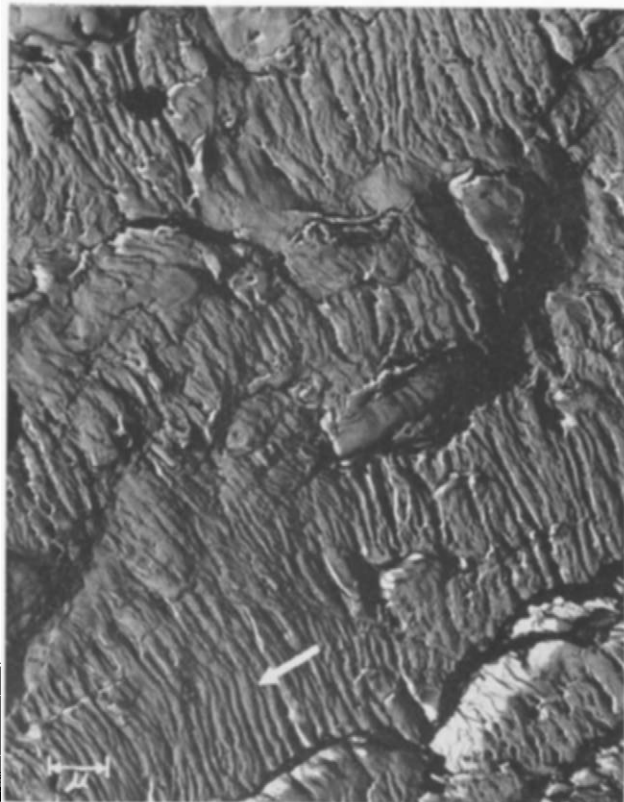
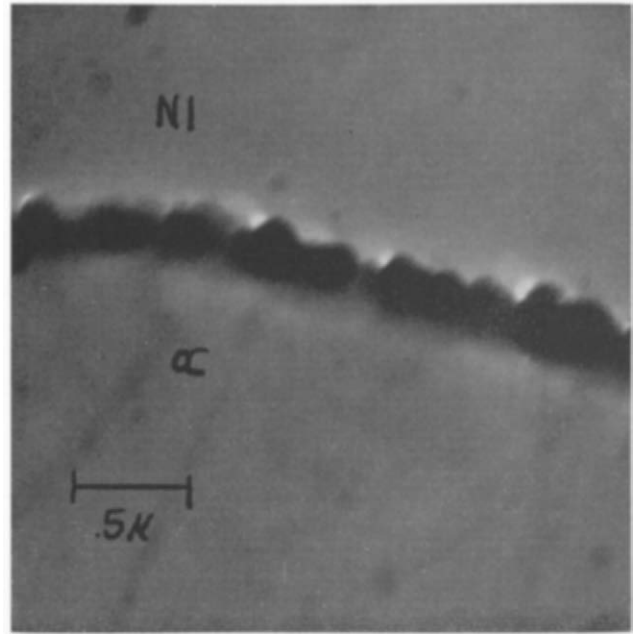
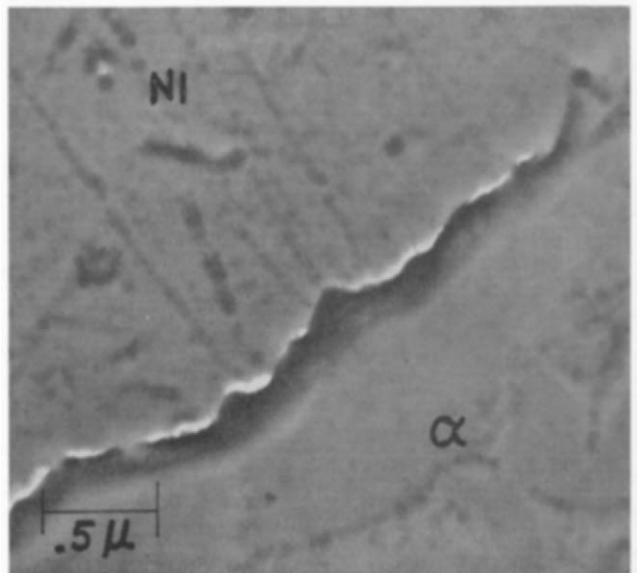


Figure 12—Fractograph of well defined fatigue striations in a normalized and tempered specimen.

The fractographic appearance of Stage II fatigue behavior in the pearlitic microstructure is considerably different than for the martensitic structure. Pearlite plus ferrite displays fairly well formed striations while martensite has ill defined and almost unrecognizable striations. This finding is in agreement with investigations in wrought steels; discernible striations have been found in mild steels while little or none were observed in high strength steels. Austenitic stainless steels, aluminum and other face centered cubic metals develop very well defined fatigue

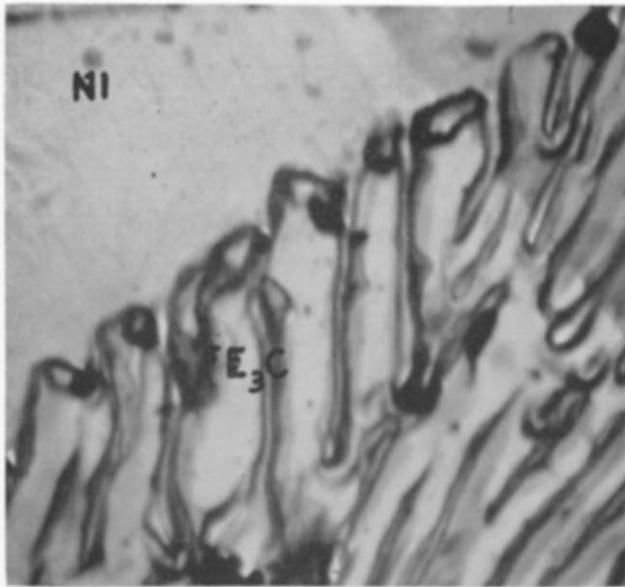


a. Ductile appearing striations.

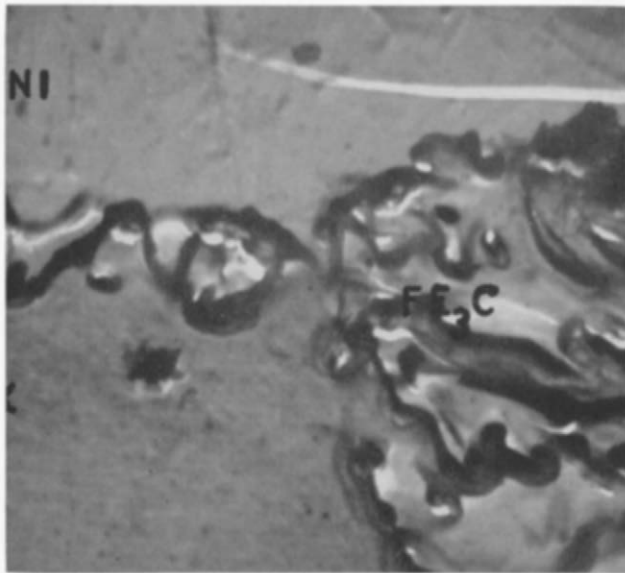


b. Brittle appearing striations.

Figure 13—Electron micrographs of cross section of fatigue striations in ferrite for a normalized and tempered specimen. Ni—nickel plated fractured surface, nital etch.



a. Cross section in pearlite.



b. Cross section in pearlite and ferrite.

Figure 14—Electron micrographs of cross section of fracture surface in normalized and tempered specimen. Ni-nickel plated fractured surface, nital etch.

striations. This suggests that the appearance of striations depends in part on the crystal structure of the metal and these metals display the clearest striations while other crystal structures produce less well defined striations.

Fatigue striations have not been found in all Stage II areas. Investigators generally agree that the crack can propagate by a number of other mechanisms, as is evidenced by areas that appear to be cleaved, areas of ill defined striations, etc. One such mechanism reported in the literature is "tear dimples." (See Figure 17.) A fair amount of plastic deformation resulting from high testing

stress and low number of cycles to failure has been identified in the early stages of crack propagation, manifested by the so-called tear dimples.

The main crack front consists of a number of local cracks separated by tear ridges and areas of cleavage. The direction of propagation varies on a local scale, i.e., the different local cracks do not necessarily propagate parallel to each other.

Stage III

The change from Stage II to Stage III is manifested by an obvious change in the roughness and appearance of the fracture surface. This has been

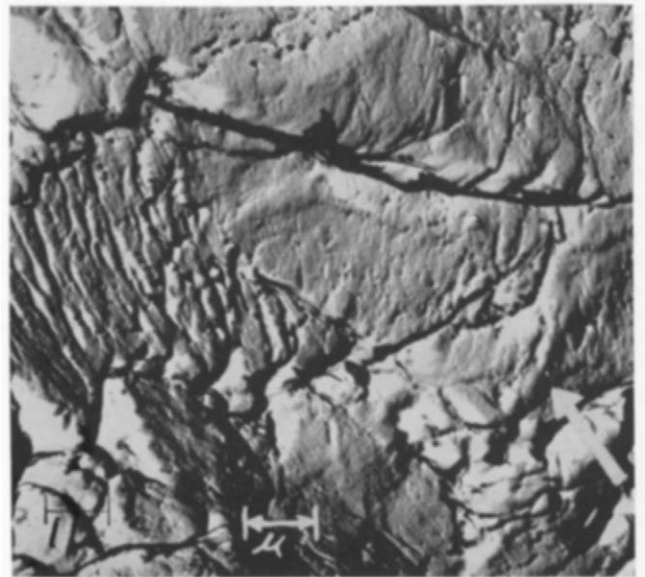


Figure 15—Fractograph of fatigue striations in quenched and tempered cast steel.

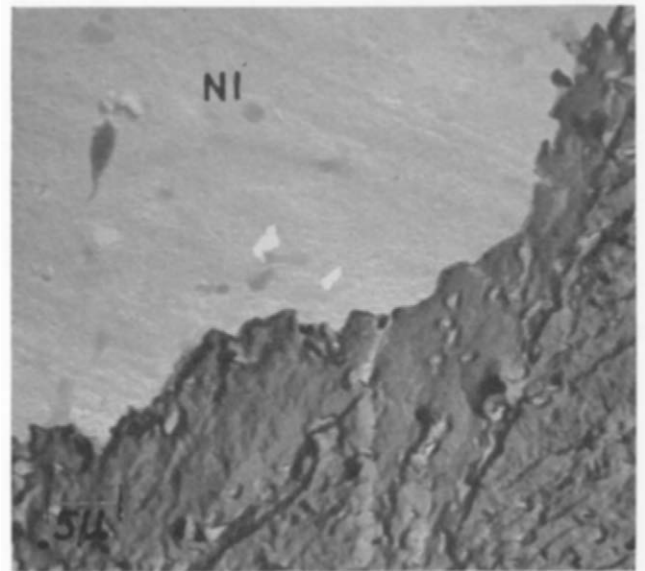


Figure 16—Electron micrograph of cross sections of fatigue striations in martensite. Ni-nickel plated fractured surface.



Figure 17—Fractograph of final failure, or Stage III, area showing dimpled rupture for normalized and tempered cast steel.

termed the pulling off stage and occupies just a few cycles until final fracture takes place. Fatigue striations are seen surrounded by areas of elongated dimples and finally the area is covered with "dimples." These "dimples" are the result of a failure mechanism known as microvoid coalescence which is common to overload failures in metals. The microvoids probably are nucleated at grain boundaries, subgrain boundaries, inclusions, or any site where a strain discontinuity exists. As the stress increases, the microvoids coalesce and eventually form a fracture surface. Figures 17 and 18 display the typical dimpled rupture appearance of Stage III for pearlite plus ferrite and martensite microstructures in cast steel. A considerable difference exists in the fractographic appearance of these two structures.

Rate of Crack Propagation and Sensitivity to Crack Initiation

The rate of crack propagation versus crack depth was investigated for notched and unnotched normalized and tempered specimens and notched and unnotched quenched and tempered specimens. Figures 19 and 20 illustrate the effect of heat treatment, notched versus unnotched specimens and crack depth on the rate of crack propagation for the Ni-Cr-Mo cast steel.

Stage II was considered to have started at the point where striations were first visible. The number of total cycles counted might well be a minimum since some of the striations near the crack initiation site may have been rubbed off during crack propagation.

The comparisons that can be made from Figures 19 and 20 are: (1) The normalized and tempered steel exhibits better fatigue life than the quenched and tempered steel. Also, the rate of crack propagation at equal crack depth is greater at equal testing stresses in the normalized microstructures. (2) The notched specimens show that the total crack lengths are, in general, shorter than the unnotched specimens. This occurs because of the multiple crack initiation sites around the edge of the specimen producing final failure in the center.

A further correlation of the greater rate of fatigue crack propagation in the normalized and tempered microstructure than in the quenched and tempered condition is shown in Figure 21. The relative rate of crack propagation for notched bar testing is also shown in Figure 21. It is interesting to note that at the 0.01-inch crack depth, there is no significance in the crack propagation rate for quenched and tempered steel whether the steel was severely notched or unnotched.

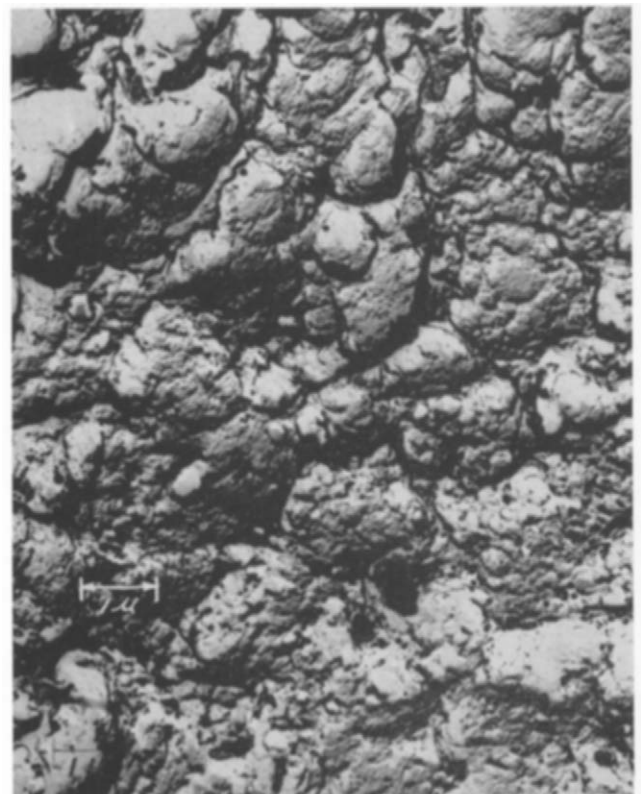


Figure 18—Fractograph of final failure, or Stage III, area showing dimpled rupture for quenched and tempered cast steel.

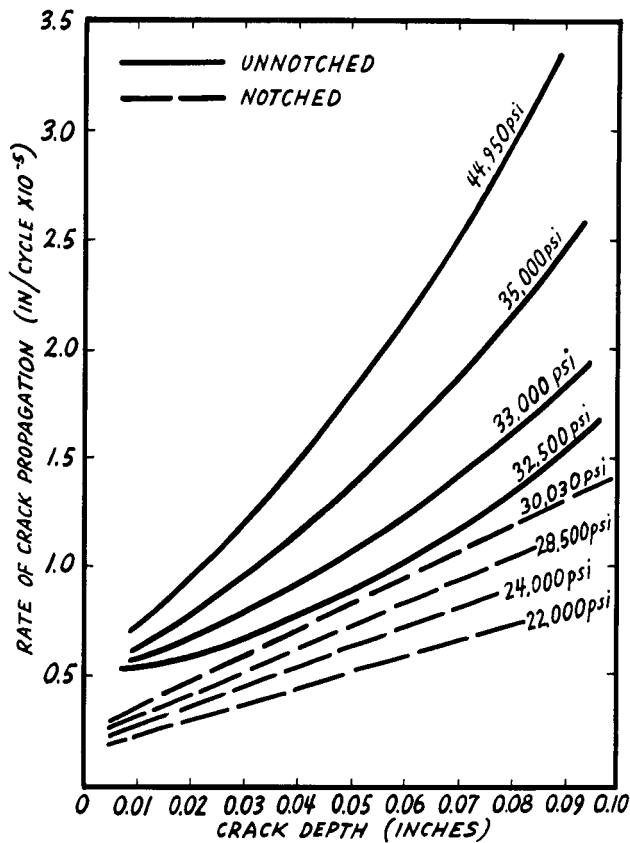


Figure 19—Effect of initial testing stress and crack depth on rate of crack propagation for normalized and tempered 83,100 psi tensile strength cast Ni-Cr-Mo steel.

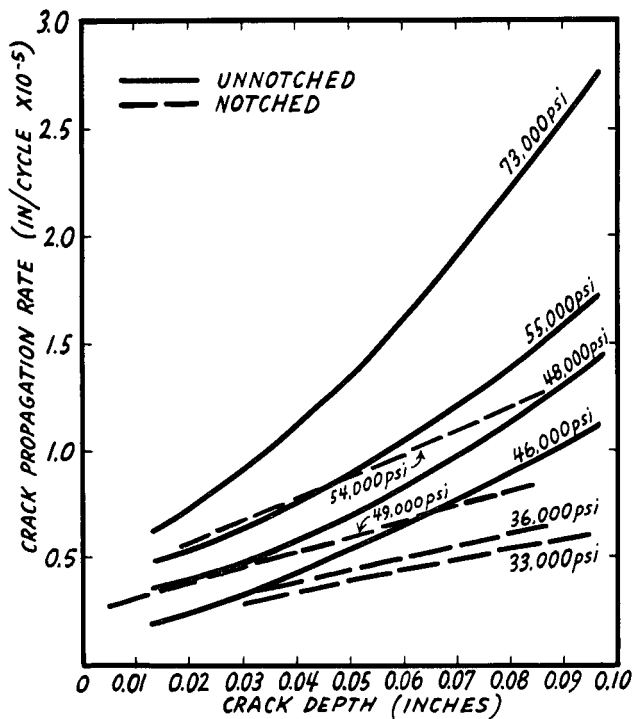


Figure 20—Effect of initial testing stress and crack depth on crack propagation rate for quenched and tempered 145,000 psi tensile strength cast Ni-Cr-Mo steel.

Steels of Equal Strength but Different Heat Treatment . . . A single heat of Ni-Cr-Mo cast steel (No. 10) was divided into two lots for heat treatment to equal tensile strengths so that the relative fatigue performance of the two microstructures could be studied further. The normalized heat treatment produced a steel of 109,000 psi tensile strength and the quenched and tempered heat treated steel gave a tensile strength of 107,000 psi. These steels were tested in fatigue (R. R. Moore unnotched specimen) at equal testing stresses as shown in Table 7. Figure 22 shows S-N curves for the 10-N and 10-QT steels.

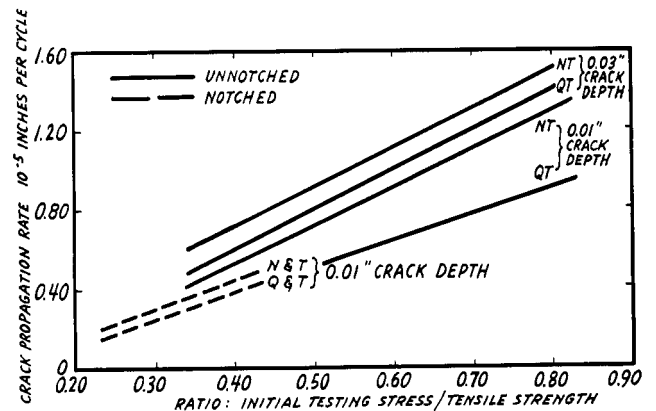


Figure 21—Effect of heat treatment on crack propagation rate at two crack depths for notched and unnotched specimens.

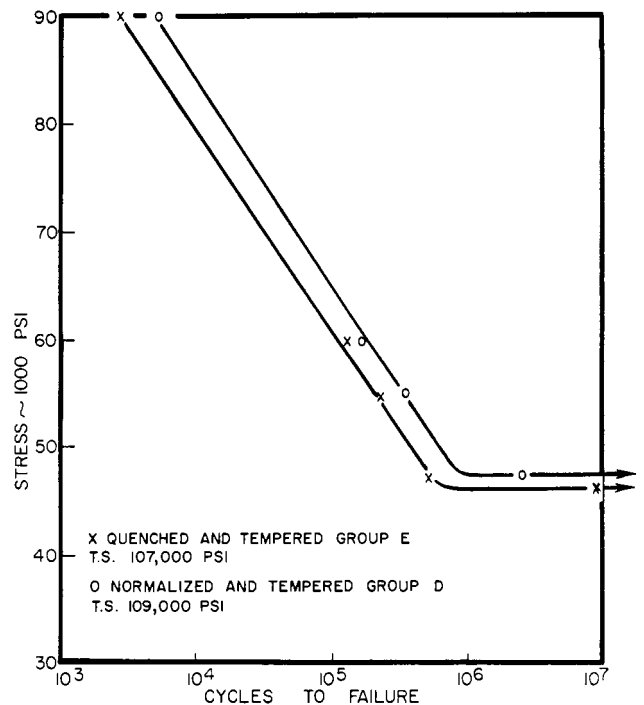


Figure 22—S-N plot for two heat treatments of nearly equal tensile strength at equal testing stresses.

TABLE 7

Fatigue Testing Stress and Life to Crack Initiation for Ni-Cr-Mo Cast Steel

Specimen Identity	Testing Stress psi	Cyclic Life	Total Cycles Counted	Life to Crack Initiation-%
7-NT-S	44,950	56,000	6,510	88.4
	35,000	529,000	9,880	98.3
	33,000	3,336,000	12,580	99.6
	32,500	5,417,000	13,330	99.8
	32,000	Endurance Limit		
7-NT-N	30,030	298,000	17,900	94.0
	28,500	448,000	17,360	96.1
	24,000	946,000	23,840	97.5
	22,000	3,455,000	30,720	99.1
	21,000	Endurance Limit		
6-QT-S	73,000	75,000	9,100	87.9
	55,000	351,000	12,780	96.4
	48,000	974,000	16,050	98.4
	46,000	1,264,000	20,450	98.4
	47,000	Endurance Limit		
6-QT-N	54,900	52,000	15,500	70.2
	49,000	140,000	18,180	87.0
	36,000	742,000	40,380	94.6
	33,000	2,051,000	45,900	97.8
	31,500	Endurance Limit		
10-N-S	55,000	360,000	11,540	96.8
	90,000	5,500	—	—
	60,000	179,000	—	—
	47,500	2,863,000	13,600	99.5
10-QT-S	55,000	229,000	12,600	94.5
	90,000	2,800	—	—
	60,000	138,000	—	—
	47,500	547,000	16,110	97.0

NT - Normalized and Tempered
 QT - Quenched and Tempered
 S - Unnotched R. R. Moore Specimen
 N - Notched R. R. Moore Specimen

The normalized cast steel exhibited better fatigue life than the quenched and tempered cast steel in all cases of equivalent testing stresses. The effect of heat treatment and crack depth on the rate of crack propagation is shown in Figure 23. The rate of crack propagation at equal crack depths is greater at equal testing stresses in the normalized microstructure. The specimens tested at 90,000 and 60,000 psi developed multiple crack initiation sites that resulted in very short crack depths to failure.

Life to Start of Cracking . . . The percent of life to crack initiation was determined by calculating the area under the curve of striation per inch versus crack depth. This figure and the total cycles to failure were used to calculate the percentage. A typical striation count versus crack depth plot for normalized and tempered Ni-Cr-Mo cast steel in the unnotched condition is shown in Figure 24.

The effect of heat treatment on the percent of life spent in initiating the crack for notched and unnotched specimens is shown in Figure 25 with the testing stress expressed as percentage of ten-

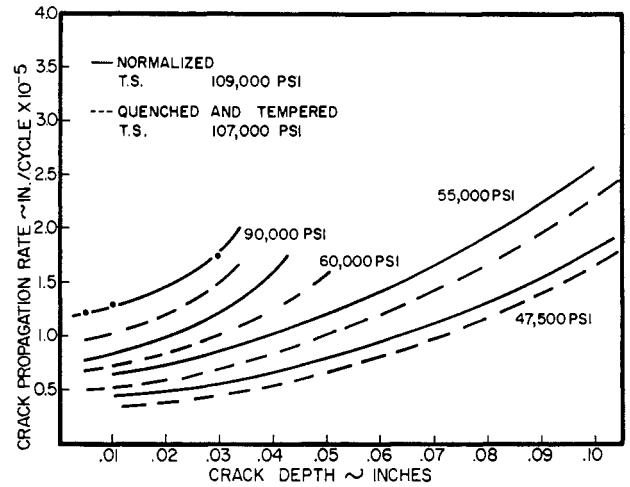


Figure 23—Effect of initial testing stress and crack depth on crack propagation rate for two heat treatments of nearly equal tensile strength at equal test stresses.

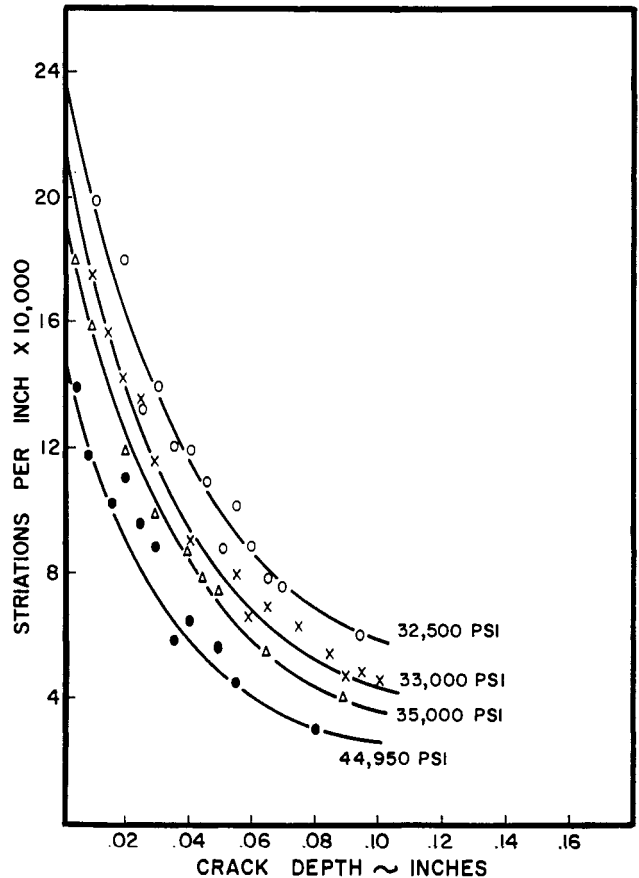


Figure 24—Effect of initial testing stress and crack depth on striation count for unnotched normalized and tempered Ni-Cr-Mo cast steel.

sile strength. The lower testing stress over tensile strength ratios and reduced percentages of life to crack initiation for the notched specimens in relation to the unnotched specimens was to be expected and is due to the notch effect.

It is also observed from Figure 25 that the quenched and tempered steel shows a greater

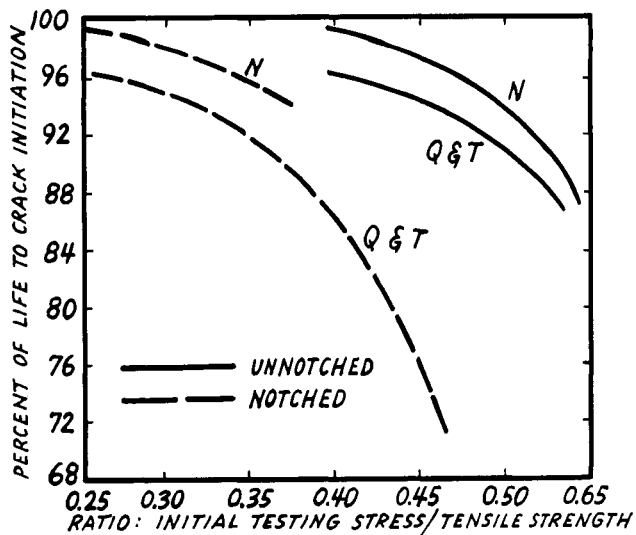


Figure 25—Effect of heat treatment on percentage of life to crack initiation for unnotched specimens.

sensitivity to crack initiation than the normalized steel at both equal strength and testing stresses and at widely divergent tensile strengths when the testing stress is expressed as percentage of tensile strength. For the nearly equal strength material, the crack initiated 2.3 to 2.6 percent of the cyclic life sooner in the quenched and tempered steel than in the normalized steel. This earlier initiation accounts for the shorter fatigue lives of tempered martensite compared to the pearlitic structure of similar tensile strength. Although the crack propagates faster in the normalized microstructure, it initiates later in cyclic life than in the quenched and tempered structure; this later initiation accounts for the better fatigue life of the former. However, the sensitivity to fatigue crack initiation was found to be greater in the quenched and tempered microstructure. Therefore, under conditions which will initiate a fatigue crack very early in life, the quenched and tempered microstructure will provide the best fatigue life.

The normalized microstructure would result in the better fatigue life under those conditions which do not initiate fatigue cracks early in life. The relatively sharp 0.015-inch radius notch does not constitute a fatigue crack, as is shown by the percentage of life spent in crack initiation for these specimens. If a sharp enough notch could be placed in the R. R. Moore specimen, the fatigue performance of the tempered martensitic structure should be better than that for the pearlitic structure.

An important observation can be obtained from the percent of life to crack initiation data for the unnotched specimens. Only for very low cyclic life tests does a crack of an appreciable size occur

early in the life of the specimen. For cyclic lives in excess of 100,000 cycles, less than ten percent of the total life is spent in crack propagation for both microstructures. A change in the steel or test conditions that influences the rate of crack propagation for this type specimen has little effect on the over-all fatigue life of the specimen. For a total cyclic life of 100,000 cycles, a decrease in crack propagation rate of 50 percent would change the over-all fatigue life by only 2.5 percent. It is, however, very important to note that this behavior is for smooth laboratory fatigue specimens and cannot be applied directly to other structures. Different kinds of specimens or structures that operate in the presence of mechanical notches or stress raisers may nucleate Stage II crack propagation much sooner in their life cycle than would be expected from these results with unnotched tests.

Effect of Inclusions

The effect of microscopic inclusions on the rate of fatigue crack propagation has not been clearly established to date. It has been stated⁽¹⁵⁾ that inclusions can produce a small crack ahead of the main crack and, thereby, accelerate the crack propagation rate. Another investigation⁽²⁵⁾ has shown that microscopic inclusions slow down the crack propagation rate by reducing the sharpness of the crack tip or by acting as crack arresters.

Microscopic inclusions did not appear to a large extent in the specimens investigated in this study. However, when they did appear, it was observed that local cracking from these particles accelerated the propagation of the crack front. Figure 26 displays typical microscopic inclusions at which the local fatigue striations have advanced ahead of the neighboring crack front and therefore, it seems apparent that the local crack front is accelerated by microscopic inclusions.

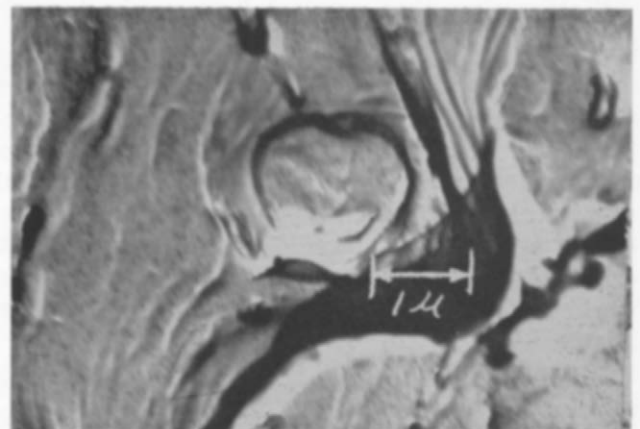


Figure 26—Fractograph of microscopic inclusion showing its effect on fatigue striations.

CONCLUSIONS TO PART II OF THE RESEARCH REPORT

The following are the conclusions resulting from this study of cast steels.

1. The rate of Stage II fatigue crack propagation in a normalized cast steel microstructure of ferrite and pearlite as determined from striation spacing is greater than in the quenched and tempered cast steel at both equal strength and testing stresses and at widely differing strengths when the testing stress is expressed as percentage of tensile strength.

2. The quenched and tempered cast steel has a greater sensitivity to Stage I crack initiation than the normalized steel. This behavior is observed at both equal strength and testing stresses and at widely differing strengths when the testing stress is expressed as percentage of tensile strength.

3. Less than ten percent of the total cyclic life is spent in Stage II crack propagation for rotating

bending fatigue specimens of the R. R. Moore type with a life cycle over 100,000 cycles.

4. The effect of brittle inclusions is qualitatively shown to increase the rate of crack propagation.

5. Fatigue striations are well defined in the normalized cast steel and less well defined in the quenched and tempered cast steel. In general, these cast steel microstructures exhibit better defined striations than those of comparative wrought steels.

6. The areas of crack initiation display no special fractographic features but discontinuities found in these areas may well be involved with crack initiation.

7. Fatigue striations are well defined in cross sections of ferrite but are less easily distinguished in the pearlite and martensite microconstituents.

APPENDIX I PREPARATION OF REPLICAS

Since the fracture surfaces were of the most importance in this study, great care was exercised in the handling of the fractured surfaces and in their preparation for replication. Surfaces not to be immediately replicated were coated with a clear plastic spray to prevent rust and contamination. Prior to replication, the surfaces were ultrasonically cleaned in an acetone solution.

The replicas were made with a two stage cellulose acetate film technique similar to that reported in the literature.⁽²²⁾ A negative of the fracture surface was made by placing a 0.005-inch-thick cellulose acetate strip, wet with acetone, firmly against the fracture surface and holding it for three minutes. The excessive use of acetone resulted in the formation of vapor bubbles at the plastic metal interface, so extreme care was required to prevent artifacts in the finished fractograph. This strip, after complete drying, was stripped from the surface with a pair of tweezers. The first two or three negatives were generally unusable because of a pick-up of dirt, loose particles of metal, etc. Negatives were checked for surface detail with a low power magnifier. The negative was then placed on a glass slide with the impression side up.

A thin layer of electron dense chromium metal was evaporated under vacuum at an oblique angle

onto the negative surface to improve the contrast of the fractographs. A vacuum of at least 10-4mm Hg is required or a defective replica will result. For this work the angle was 45 degrees and the direction that of crack propagation. This "shadowing" was accomplished by passing a heating current through a filament of tungsten wire wound into a loose coil with chromium chips inside.

A layer of carbon was then deposited uniformly onto the surface by complete evaporation of a 1 mm (0.039 inch) diameter and 1 cm (0.39 inch) long carbon rod. A current of 50 amperes was passed through the rods for periods of 0.5 seconds. A drop of oil on a white ceramic block placed near the replica was used to estimate the thickness of the layer deposited. A diagram of the bell jar arrangement used for this work is shown in Figure 27. A replica which was 150 to 200 angstroms thick provided the best results.

The cellulose acetate backing was removed from the replica by dissolving it carefully in acetone. This was accomplished by placing the replica on a 200-mesh specimen grid and both of these on a fine stainless steel screen. The screen was then lowered until it barely touched the surface of an acetone pool. The replica was left in the acetone for four periods of fifteen minutes, drying the screen between each period by blotting a number

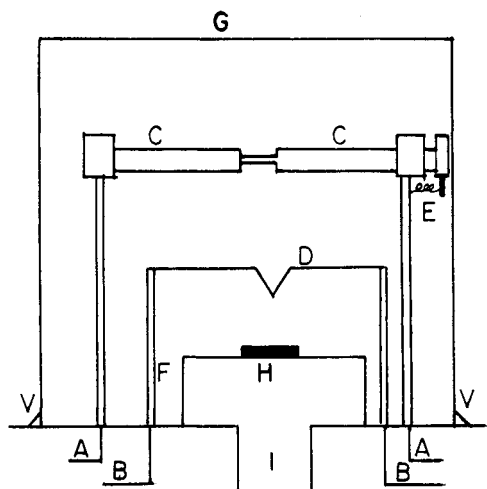


Figure 27—Evaporating unit—

- a. Electrical leads to carbon rods (for carbon evaporating)
- b. Electrical leads to tungsten filament (for chrome shadowing)
- c. Carbon rods
- d. Tungsten filament (set back from plane of drawing to give 45° shadowing angle)
- e. Spring to maintain contact of carbon rods
- f. Specimen stand
- g. Glass bell jar
- h. Specimen
- i. To vacuum pumps
- v. Vacuum seal

of times on filter paper. The replica was then ready for viewing in the electron microscope. All fractographs in this report were taken on a RCA type, EMU2 electron microscope.

Micrographs of polished and etched cross sections were prepared by first depositing a hard nickel plate on the fracture surface. The specimen was then ground and polished to the area in question. After a light nital etch, the surface was replicated by dropping a solution of one percent collodion in amyl acetate onto the surface. When the material became tacky, a 200-mesh microscope grid was placed over the area in question. After complete drying, the area was scribed off with a sharp tool. The surface was then moistened with breath and the negative and grid peeled off with scotch tape. The balance of the technique is the same as for the cellulose acetate method except that the solvent used to dissolve the backing was amyl acetate.

Rate Study Methods

The rate of crack propagation was studied by counting the number of striations per inch at a

number of places, beginning at the point of crack initiation and proceeding directly to the point of final failure. It was difficult to correlate the fractograph exactly at the point on the fracture surface from which it was taken.

The problem of finding the crack length at any particular area has been solved in two ways. It was found that the 200-mesh specimen grid was very uniform in the dimensions of its grid openings. The distance from center to center of the square openings is 0.005 inch. From a replica of the whole surface, a narrow strip, approximately 0.04 inch wide, was cut with specimen shears. One end of this strip was located at the apparent point of crack initiation and the other end at the final failure area. This was carefully aligned on a specimen grid parallel with the rows of openings, as shown in Figure 28. One grid can accommodate a strip 0.11 inch long, so a large percentage of the crack propagation path can be accommodated in this way. An accuracy of plus or minus 0.003 inch in crack length has been reported by this method without external marking methods.⁽²³⁾

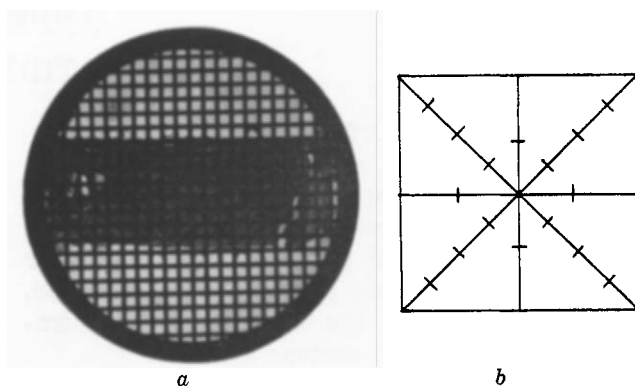


Figure 28—Methods used for determination of the rate of crack propagation from striation spacing.

- a. Replica of fracture path aligned on electron microscope sample grid, 24X
- b. Sketch of target used for counting striation spacing

An alternate method of scratching lightly on the fracture surface and measuring the distance from the crack origin to the scratch was also used. The scratch was then replicated and a number of readings of striations per inch were taken near the scratch. The average of these readings was plotted at the crack depth of the scratch. The former method was used near the point of crack initiation and the latter for areas near final failure. In the first method, the center two lines of grid openings were studied by counting the striation spacing at a number of places in each grid opening and averaging the results at the crack

depth corresponding to the center of the opening. The results for both rows were averaged for the final data point. In this way, each point represents from 10 to 15 readings. In the second method, several readings were taken on either side of the scratch and the average was plotted at the crack depth of the scratch.

To accomplish the counting of striation spacing,

a graduated target was prepared on the fluorescent viewing screen of the electron microscope. A copy of this target is shown in Figure 28. Since the image revolves as the magnification is incrementally changed, one of the graduated lines in the target can be positioned perpendicular to any group of striations and the striations per inch and inches per cycle can be calculated after the magnification of the image has been established.

REFERENCES TO PART II

1. Forrest, P. G., *Fatigue of Metals*, Pergamon Press, New York, 1962, p. 2.
2. Wulpi, D. J., "Characteristics of Fatigue Fractures," *Metal Progress*, Vol. 89, 1966, p. 79.
3. Lessels, J. M., *Strength and Resistance of Metals*, New York, 1954, p. 300.
4. Peterson, R. E., *Handbook of Experimental Stress Analysis*, John Wiley, New York, 1950, p. 593.
5. Zappfe, C. A., and Wordon, S. O., "Fractographic Registration of Fatigue," A.S.M. Preprint, 1950.
6. Zappfe, C. A., "Hydrogen Theory for Brittle Ship Plate," *Metal Progress*, Vol. 59, 1951, p. 802.
7. Crussard, C., Borione, R., Plateau, J., Morillon, J., and Lajeunesse, K., "A Comparison of Ductile and Fatigue Fractures," *Fracture*, John Wiley, New York, 1959.
8. Forsyth, P., and Ryder, D., "Some Results of the Examination of Aluminum Alloy Specimen Fracture Surfaces," *Metallurgia*, Vol. 63, 1961, p. 117.
9. Crussard, C., Borione, R., Plateau, J., Morrillon, J., and Maratray, F., "A Study of Impact Tests and the Mechanism of Brittle Fracture," *Journal of the Iron and Steel Institute*, Vol. 183, 1956, p. 145.
10. Gilmore, K., "Advances in Electron Microscopy," *Electronics World*, Vol. 70, July 1965, p. 21.
11. Forsyth, P., and Ryder, D., "Fatigue Fracture," *Aircraft Engineering*, Vol. 32, No. 374, 1960, p. 96.
12. Laird, C., and Smith, G., "Crack Propagation in High Stress Fatigue," *Phil. Mag.*, Vol. 7, 1962, p. 847.
13. Manson, S., "Fatigue- A Complex Subject - Some Simple Approximations," *Experimental Mechanics*, Vol. 5, July 1965, p. 196.
14. Jacoby, G., "Fractographic Methods in Fatigue Research," *Experimental Mechanics*, March 1965, Vol. 5, p. 65.
15. Forsyth, P., "A Two Stage Process of Fatigue Crack Growth," in *Symposium on Crack Propagation*, Cranfield, England, September 1961, p. 75.
16. Forsyth, P., and Stubbington, C., "The Slip-Band Extrusion Effect Observed in Some Aluminum Alloys Subjected to Cyclic Stresses," *Journal Institute Metals*, Vol. 83, 1954, pp. 395 - 399.
17. Grosskreutz, J., and Shaw, G., "Mechanism of Fatigue in 1100-0 and 2024-T4 Aluminum," *Midwest Research Inst., Tech. Rept. AFML-TR-65-127*, July 1965.
18. Head, A., "The Growth of Fatigue Cracks," *Phil. Mag.*, Ser. 44, 1953, p. 925.
19. Laird and Smith, p. 853.
20. Jacoby, G., "Observation of Crack Propagation on the Fracture Surface, Current Aeronautical Fatigue Problems - Symposium, Pergamon Press, New York, 1963, p. 180.
21. Hertzberg, R., "Application of Electron Fractography and Fracture Mechanics to Fatigue Crack Propagation in High Strength Aluminum Alloys," Ph.D. Dissertation, Lehigh University, May 1965.
22. Scott, R., and Turkalo, A., *Proc. of ASTM*, Vol. 57, p. 536.
23. Pelloux, R., "The Analysis of Fracture Surfaces by Electron Microscopy," *Metals Engr. Quarterly*, Vol. 5, No. 1965, p. 26.
24. Forsyth, P., "Fatigue Damage and Crack Growth in Aluminum Alloys," *Acta Met.*, Vol. 11, No. 7, 1963, p. 703.
25. McEvily, A., "Effect of Constituent Particles on the Notch Sensitivity and Fatigue Crack Propagation Characteristics of Al-Zn-Mg Alloy," NASA, TD D-328, April 1962.

**STEEL FOUNDRY RESEARCH FOUNDATION
Published Research Reports***

Recommended Practice for Repair Welding and Fabrication Welding of Steel Castings, 58 pages	\$.50
Studies of the Design of Steel Castings and Steel Weldments as Related to Methods of their Manufacture, 47 pages	\$.35
Effect of Shrinkage Porosity on Mechanical Properties of Steel Casting Sections, 16 pages	\$.40
Correlation of Destructive Testing of Steel Castings with Stress Analysis and Mechanical Properties	
Part I-A Summary Report, 20 pages	\$.50
Part II-The Detailed Report, 50 pages	\$ 2.50
The Effect of Surface Discontinuities on the Fatigue Properties of Cast Steel Sections, 28 pages	\$.50
The Evaluation of Discontinuities in Commercial Steel Castings by Dynamic Loading to Failure in Fatigue, 44 pages	\$.50
Fatigue of Cast Steels. Part I-A Study of the Notched Effect and of the Specimen Design and Loading. Part II-Fractographic Studies, 28 pages	\$.50

* Available to the public at the price shown-Minimum billing \$1.00

**STEEL FOUNDRY RESEARCH FOUNDATION
21010 Center Ridge Road Rocky River, Ohio 44116**